Advances in Science and Technology Research Journal

Advances in Science and Technology Research Journal, 2026, 20(10), 311–327
https://doi.org/10.12913/22998624/225399
ISSN 2299-8624, License CC-BY 4.0

Received: 2026.05.27
Accepted: 2026.07.13
Published: 2026.09.01

Enhancing the uniformity of surface quality across various orientations of fused deposition modeling components using a hybrid Taguchi fuzzy model

Amjad B. Abdulghafour[1], Samah A. Aufy[1*], Rasha Qasim Humadi[2], Waad Q. Shiaa[1]

[1] Production Engineering and Metallurgy College, University of Technology, Baghdad, Iraq
[2] Ministry of Education, Gifted Guardianship Committee, Baghdad, Iraq
* Corresponding author's e-mail: samah.a.alkhalidy@uotechnology.edu.iq

ABSTRACT

As a leading additive manufacturing technology (AM), fused deposition modeling (FDM) exhibits exceptional versatility in processing a wide range of thermoplastic polymers for industrial applications. Nonetheless, achieving optimal part quality is inherently governed by a multitude of process variables, the intricate relationships of which dictate the final structural and functional performance. The consequence is that measuring 3D printed components has metrological limitations that are inherent to the layer-by-layer material extrusion process and strongly influenced by thermal shrinkage gradients and the anisotropic behavior of the deposited material during the printing process. Thus, this study developed a Taguchi – fuzzy logic model (T – FLM) as a hybrid model that aims to enhance the surface quality of the printed parts, thereby ensuring uniform surface characteristics across complex components, especially including rotational, horizontal, vertical, and inclined surfaces. The specimen geometry was specially designed to feature these distinct characteristics. The orthogonal array (OA) L_{27} experiments were conducted using PLA material. Experimental design parameters included layer thickness, nozzle temperature, print speed, bed temperature, and top/bottom layer number. The developed model utilized the experimental design to determine the responses of surface roughness (Ra) and deviation in dimensional accuracy (), which were subsequently formulated into the multi–response performance index (MRPI) for optimization. The results confirmed the effectiveness of the hybrid model in optimizing the targeted response, wherein the enhanced uniformity in the printed parts' surface quality was statistically quantified through central tendency and variability indices. This was evidenced by the statistical analysis of the fuzzy model, which consistently yielded elevated MRPI values across all 27 experimental runs, achieving a notable improvement of 15.2%. Furthermore, a distinct improvement in the standard deviation of the overall surface quality was successfully demonstrated in approximately 78% of the runs. Additionally, an analysis of variance (ANOVA) test was performed to identify the statistically significant process parameters, and the validity of the optimal combination was successfully verified through a confirmation test. In conclusion, the developed model proved highly capable of maintaining uniform surface quality across various geometric orientations, thereby establishing a robust model that overcomes the limitations of the traditional approach.

Keywords: FDM, surface roughness & dimensional accuracy, multi-response performance index, fuzzy logic.

INTRODUCTION

Competitive market is essential for product development, enhancing product quality and production flexibility. A noticeable trend in certain market segments is the shift away from mass production in favor of small-scale customized manufacturing. To meet evolving demands, rapid prototyping (RP) is utilized as an advanced technology to transform virtual designs into physical components with complex geometrical challenges using additive manufacturing (AM) processes, rather than traditional subtractive technologies. This method allows for printing geometric complexity while ensuring faster production and improving cost-effectiveness. This enables and facilitates proactive design verification and incremental iterative refinement during preliminary stage of development before full-scale implementation [1,2]. Several AM technologies have been developed and refined over years, which are categorized as liquid, solid, and, powder-based products. This presents distinct advantages, necessitating a selection process guided by the material type, resolution standard, and mechanical performance criteria [3,4]. The FDM process is one of the AM technologies generally used to fabricate components from three-dimensional (3D) model data, in which a filament is heated and then the material is deposited via a nozzle onto the build bed [5]. The thermoplastic filament is heated to its melting point and extruded layer-by-layer to construct the desired part [6]. The measurements of the printed parts are characterized by metrological challenges due to extrusion material in form layer – by – layer and thermal gradient during printing process, so that it exhibits inclined surface greater roughness and deviation dimensions compared the flat ones [7,8]. Since real–world applications often involve complex geometries with diverse surface orientations, it is significant to comprehensively assess the surface quality across different surface orientations [9]. Surface quality is a key determinant of product quality and mostly specified as a vital technical requirement in manufacturing of mechanical parts. Thereby, it is essential to achieve mechanical performance through geometric interlocking, sealing, or surface contact to enhance frictional resistance and extend service life. It enhances the aesthetic appeal and the accurate functioning of precision engineered components compared to machining methods [10,11].

Recently, the literature review has highlighted the evolution of the FDM technology from rapid prototyping to a high-performance manufacturing process. Research efforts often focus on optimizing the mechanical properties of printed parts, while modern studies incorporate AI techniques for addressing real–time monitoring and predictive modeling in achieving industrial–grade precision. Sammaiah et al. (2020) [12] introduced the effect of two controllable process parameters, infill layer height and infill density, on the surface roughness of ABS material. The obtained results proved that the surface roughness increases with a larger infill layer height at each level of infill density. Trivedi et al. (2020) [13] presented a hybrid methodology for predictive modeling in 3D printing. A fuzzy logic-based system was developed to estimate tensile strength. Experimental results indicated that the superior strength is achieved with lower part orientation, elevated extrusion temperature and increased layer thickness. Utilizing Taguchi method for empirical testing, a comparative analysis was conducted between the fuzzy logic predictions and experimental data. This study demonstrated strong alignment among the computational numerical and experimental evaluations of tensile strength. Syed et al. (2022) [14] developed a Grey-Taguchi approach to optimize the FDM process parameters, including layer thickness, raster angle, infill density, number of contours, printing temperature, and printing speed. Taguchi L_{27} OA was selected as the statistical design of experiments approach to systematically evaluate the behavior of the FDM process. ANOVA was subsequently performed to quantify the percentage contribution of impact of each input factor on the multiple performance responses. Multi-objective optimization was executed using gray rational analysis. The optimal parameter configuration that simultaneously minimized longitudinal shrinkage while maximizing both tensile and flexural strengths was determined to be: a layer thickness of 0.2 mm, 90° raster angle, an infill density 30%, 16 contours, a printing temperature 230 °C, and a printing speed 60 mm/s. Hasdianah et al. (2023) [15] used the Taguchi method in studying the impacts of 3D printing process parameters on the surface roughness of TPU material. The experimental framework examined six key parameters, namely flow rate, layer thickness, nozzle temperature, print speed, overlap, and fan speed. Systematic optimization was achieved through the Taguchi L_{27} design, evaluated alongside signal to noise ratio (S/N) and ANOVA. Furthermore, linear regression analysis was applied to characterize the empirical relationships between process inputs and the resulting surface topography. The results reveal that the layer thickness is the most dominant factor regulating surface roughness, yielding a substantial percentage contribution of 65.11%. Finally, validation via a confirmation test demonstrated strong agreement between the experimental results and the statistical predictions. Deswal et al. (2024) [16] presented a hybrid evolutionary algorithm to optimize input process parameters and compressive strength by integrating genetic algorithm and fuzzy logic model. The finding was demonstrated optimization of the compressive strength with (49.7303 MPa) compared experimental (47.08 MPa) and fuzzy predicted (47.101 MPa) value. Abdulridha et al. (2024) [17] presented a systematic approach to improve mechanical characteristics and geometric dimensions of the 3D printed parts, which are made from polyethylene terephthalate glycol (PETG) materials. The obtained outcomes illustrate the effects of the process parameters under study, namely infill line distance, wall line count, and build plate temperature affecting the inherent characteristics of the printed parts. EL-Zathry et al. (2026) [1] developed an ANN model to predict optimum surface roughness (SR) of the FDM-produced parts across different orientations. This model demonstrated consistent improvement of surface roughness across horizontal, vertical and inclined orientations. Among the various process parameters in FDM, surface orientation plays a vital role in specifying the final product quality; it creates a critical trade – off between aesthetic quality and geometric accuracy. It directly influences the staircase effect, which is the primary cause of surface roughness [1,11]. Moreover, the orientation determines the thermal distribution and the sequence of layer stacking, both of which significantly influence dimensional accuracy due to non–uniform shrinkage across surface orientations. Therefore, this study investigated surface orientation as a primary factor to achieve a balance between surface integrity and dimensional compliance through advanced optimization techniques [1,10]. Consequently, the inherent uncertainty of FDM operational environment necessitates a more sophisticated control over surface quality of complex geometries. To address this, the current study proposed a hybrid model that integrates the Taguchi approach with a fuzzy logic system to establish robust framework, ensuring uniformity integrity across various surfaces orientations in complex geometries.

PROPOSED MODEL AND EXPERIMENTAL FRAMEWORK

This section proposed a hybrid model that integrates the Taguchi approach and a fuzzy logic system to establish a robust experimental framework. This model simultaneously addresses conflicting manufacturing objectives in FDM parts featuring geometric complexities, thereby ensuring a balanced multi-response performance across various surface orientations rotational, horizontal, vertical, and inclined surfaces.

Sample preparation

Generally, 3D printing parameters play a vital role in determining production efficiency and the properties of the printed part particularly mechanical properties. Therefore, it is essential to study how input parameters influence the surface texture quality and the dimensional accuracy of the final geometry of the printed parts [18,19]. Each 3D printer operates with unique characteristics and specific requirements related to its operating conditions. This work was treated with a set of input parameters such as the layer thickness, nozzle temperature, print speed, bed temperature, and top/bottom number layers. Herein, the printed sample is required to design a test specimen in a special geometry with dimensions (73 × 36 × 17 mm) as illustrated in Figure 1, highlighting the investigated surface orientations in the context of FDM printed parts, such as the rotational surface (S_R) with a radius (18 mm) to the horizontal plane; it refers to a curved geometric feature generated through the continuous interpolation of the printer's X and Y axes, horizontal surface (S_H) and vertical surface (S_V) refer to specimens with their longest axis parallel and perpendicular respectively to the built plate, while inclined (S_I), which describes the created specimen's angle (45°) to the horizontal plane, which is approximated by a series of shifted layers, creating a characteristic profile known as the "staircase effect".

Experimental design

To conduct experimental investigations, all test specimens were created by a 3D printer. The machine type is Bambu Lab A1 with the specifications presented in Table 1, supporting various thermoplastic materials such as poly lactic acid (PLA) filament. PLA is grouped between the biopolymers so that its renewability and biodegradability have made it more interesting for a wide range of goods applications. Furthermore, it can be more easily processed using conventional techniques such as extrusion and compression molding and modern techniques like 3D printing [20,21]. Table 2 listed the specifications and properties of the PLA material [22].

The 3D CAD models of the specimens were designed using SOLIDWORKS Software. Then,

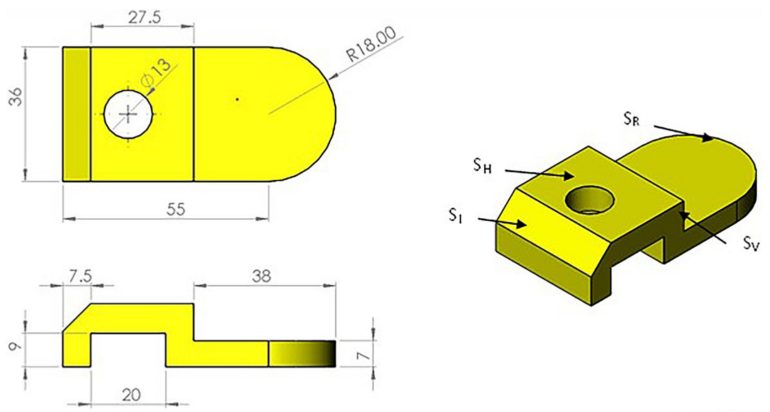

Figure 1. Test specimen Geometry

the model was exported in STL file format to be processed by the slicer Ultimaker Cura Software which slices the 3D model with the predetermined process parameters. The goal of the slicing program is to split the specimen into the desired number of layers. The result of the slicing process is a file involving the required information needed to print the part. In FDM technology, printing parameters are substantially influenced by the print quality properties of the printed parts. Thus, several challenges emerged that ultimately affected the surface integrity of the printed parts. Specifically, surface roughness (Ra) and deviation in dimensional accuracy (ΔL) that are established due to the staircase effect and thermal gradient arising during the solidification process [23].

Design of experiments (DOE) developed by Taguchi is used to determine the optimal parameter setting for each factor that directly affects the surface quality of 3D printed parts to be more robust [2]. Selection of these parameters based on preliminary trials and literature data significantly streamlines the process while ensuring the statistical validity and accuracy of the analysis. In this study, layer thickness (0.1–0.2 mm), nozzle temperature (200–220 °C), print speed (20–60 mm/sec), bed temperature (50–60 °C), and top/bottom layer number (2–6) with three levels were selected to analyze the influence of the printer parameters on the print quality of the printed results, specifically surface roughness and deviation in dimensional accuracy. In turn, orthogonal array (OA) (L_{27}) was selected and tabulated in Table 3. The actual 27 printed samples are illustrated in Figure 2a. To ensure the reliability and reproducibility of the results, surface texture analysis was performed with a Mahr MarSurf PS1 portable profilometer with precision (±0.001 μm), precisely measured the arithmetical mean roughness of the test surface. The maximum measuring range is 350 μm (-200 μm to +150 μm). The measurements were executed in accordance with the DIN EN ISO 4287 standard. The experimental setup was performed utilizing a Gaussian filter with a cut-off length (*Lc*) of 0.250 mm, resulting an evaluation length (*In*) of 1.250 mm. The stylus traverse length (*Lt*) was set to 1.750 mm. To start the measurement, the Mahr MarSurf PS1 probe was brought into contact

Table 1. Machine specification

Specification	Description
Nozzle diameter	0.4 mm
Print speed	200–300 mm/s
Nozzle temperature	Up to 300 °C
Bed temperature	100 °C
Slicer software	Cura, Suerslicer, and Prusaslicer

Table 2. PLA filament specification and properties

No.	Parameters	Values
1	Material	PLA (filament diameter: 1.75 mm)
2	Filament length	330 m
3	Spool net weight	1 kg
4	Density	1.24 g/cm³
5	Melt flow index (MFI)	6 g/10 min (190 °C/2.16 kg)
6	Heat deflection temperature (HDT)	50 °C
7	Tensile strength	62 MPa
8	Tensile elongation	4.4%
9	Flexural strength	66 MPa
10	Flexural modulus	2800 MPa
11	Impact strength	4.2 kJ/m²
12	Diameter tolerance	1.75 ± 0.05 mm

Table 3. DOE using Taguchi method based on OA (L_{27})

Exp. No.	FDM printing parameters				
	Layer thickness (mm)	Nozzle temp. (˚C)	Print speed (mm/sec)	Bed temp. (˚C)	Top/bottom layer No. (#)
1	0.1	200	20	50	2
2	0.1	200	20	50	4
3	0.1	200	20	50	6
4	0.1	210	40	55	2
5	0.1	210	40	55	4
6	0.1	210	40	55	6
7	0.1	220	60	60	2
8	0.1	220	60	60	4
9	0.1	220	60	60	6
10	0.15	200	40	60	2
11	0.15	200	40	60	4
12	0.15	200	40	60	6
13	0.15	210	60	50	2
14	0.15	210	60	50	4
15	0.15	210	60	50	6
16	0.15	220	20	55	2
17	0.15	220	20	55	4
18	0.15	220	20	55	6
19	0.2	200	60	55	2
20	0.2	200	60	55	4
21	0.2	200	60	55	6
22	0.2	210	20	60	2
23	0.2	210	20	60	4
24	0.2	210	20	60	6
25	0.2	220	40	50	2
26	0.2	220	40	50	4
27	0.2	220	40	50	6

with the surface of the specimen; the diamond stylus with a tip radius of 2µm was employed. To minimize experimental error and verify repeatability of the 3D printing process, three distinct measurements were taken per specimen surface, and the mean resultant for the surface parameter was reported; for example, horizontal surface measurement on the top was conducted because the surface roughness is accurately evaluated when perpendicular to the orientation of the print as shown in Figure 2b. Deviations in dimensional accuracy (ΔL) of the modeled specimens were measured using a digital Vernier caliper with a precision ±0.01 mm. For each run, every surface was measured five times, and the average percentage deviation was calculated using Equations 1–3 [22].

$$Deviation\ (D_i) = \left| \begin{matrix} Specified\ Diamension - \\ - Observed\ Value \end{matrix} \right| \tag{1}$$

$$Percenage\ Deviation\ (D_{pi}) = \left(\frac{D_i}{Specified\ Diamension}\right) * 100 \tag{2}$$

$$Average\ Percenage\ Deviation = \frac{D_{p1} + D_{p2} + D_{p3}}{3} \tag{3}$$

Fuzzy logic model

The Taguchi method is traditionally designed for single-response optimizing, it is based on signal – to –noise ratio (S/N) to address the effect of process parameters on responses, denoted by "η". The parameter with highest S/N ratio indicates the optimal level. Consequently, it exhibits inherent limitations

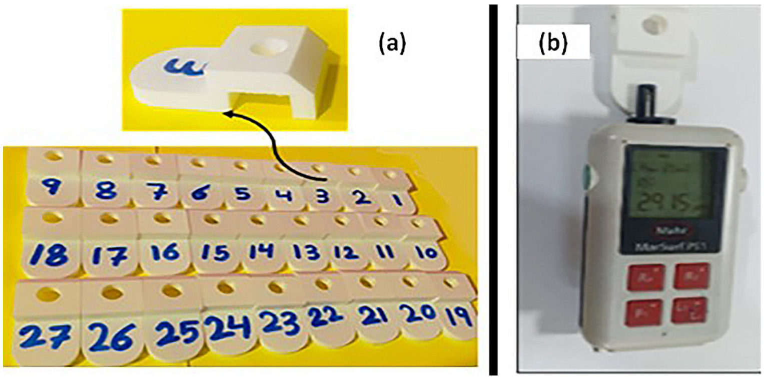

Figure 2. (a) Actual printed parts, (b) Roughness test for printed specimen

when handling multi-responses. In accordance with surface roughness and deviation in dimensional accuracy objectives, a "smaller is better" quality characteristic was established, as expressed in Equation 4.

$$\eta = -10\, log\left(\frac{1}{n}\sum_{i=1}^{n} Y_i^2\right) \tag{4}$$

where: "η" represents the S/N ratio of the ith experiment, and "Y_i" denotes the outcome value of ith experiment [24].

To overcome the limitations of the traditional Taguchi approach, a hybrid Taguchi–fuzzy logic model (T–FLM) was developed as a robust experimental framework to evaluate the performance, which can also be extended to handle multi-objective optimization via the multi–response performance index (MRPI), specifically with lower surface roughness (Ra) and deviation in dimensional accuracy (ΔL). This framework effectively addresses incomplete and imprecise information, which typically challenges conventional probability theory. The MRPI index was selected as the evaluation metric because it effectively integrates multi-response into single response [24,25]. Fuzzy logic system comprises of a fuzzifier featuring two input variables, surface roughness (Ra) and deviation in dimensional accuracy (ΔL) and one output response named multi-response performance index (MRPI). Input measurements data, expressed as S/N ratio, undergo an initial normalization step using Equation 5. Subsequently, the fuzzy system employs triangular membership functions to fuzzify both input and out variables, ensuring that the linguistic values are scaled between zero and one in accordance with Equation 6.

$$X_i{}^* = \left(\frac{x_i^0(k) - min\, x_i^0\,(k)}{max\, x_i^0\,(k) - min\, x_i^0\,(k)}\right) \tag{5}$$

where: X_i^* indicates the normalization value of η, $max\, x_i^0\,(k)$ and $min\, x_i^0\,(k)$ represent the maximum and minimum value of η_i for the ith response [24].

$$triangle\,(x; a, b, c) = \\ = max\left(min\left(\frac{x-a}{b-a}, \frac{c-x}{c-b}\right), 0\right) \tag{6}$$

where: x indicates the input variable range and a, b, and c are the linguistic value parameters [23].

A fuzzy rule base that represents input membership values as weighting factors to determine their influence on the fuzzy output sets of the final output conclusion [6,26]. Four membership functions of input have been selected, i.e., short (S), medium (M), high (H) and extremely high (EH). While five membership functions have been selected for the output i.e., low (L), medium (M), high (H), very high (VH) and excellent (E) and their boundaries tabulated in Table 4. Formation of a linguistic rule base MRPI, based on a larger S/N ratio indicating better performance characteristics, sixteen fuzzy rules are designed, as listed in Table 5. These rules are structured based on an "if-then" condition, where two input variables (S/N ratio of Ra and S/N ratio of ΔL) utilized to determine the single output variable (MRPI) as follows:

Rule #: if $\eta_{(Ra)}$ is (S) and η (ΔL) is (M) then MRPI is (L); where S, M, and L are fuzzy subsets that corresponding membership function of the fuzzy variable (i.e., µS, µM, and µL). The expressions $MRPI_{SR}$, $MRPI_{SH}$, $MRPI_{SV}$, and $MRPI_{SI}$

describe the output variables of the fuzzy model for rotational, horizontal, vertical, and inclined surfaces, respectively. The maximum-minimum combinational fuzzy reasoning rules are applied to yield a fuzzy output. Subsequently, a defuzzification process is employed to convert the fuzzy inference output into a crisp (non-fuzzy) value, denoted as the multi-response performance index (MRPI). This is achieved using the centroid of area (COA) method, as expressed in Equation 7 [23].

$$COA = \frac{\int_y \mu_D(y) y dy}{\int_y \mu_D(y) dy} \quad (7)$$

where: $\mu_D(y)$ is the fuzzy reasoning membership function of the output, and y is the output variable.

The general outline of the developed model is illustrated in Figure 3. This model was implemented and simulated using the MATLAB Software.

RESULTS AND DISCUSSION

The experimental data and step-by-step mathematical formulations involved in executing the

Table 4. Input and output variables of FLM with their fuzzy values

Linguistic variable	Linguistic value	Term set	Numerical range
S/N of Ra (INPUT)	Short	S	[0.00–0.40]
	Medium	M	[0.20–0.60]
	High	H	[0.40–0.80]
	Extremely high	EH	[0.60–1.00]
S/N of ΔL (INPUT)	Short	S	[0.00–0.40]
	Medium	M	[0.20–0.60]
	High	H	[0.40–0.80]
	Extremely high	EH	[0.60–1.00]
MRPI (OUTPUT)	Low	L	[0–000–0.332]
	Medium	M	[0.166–0.498]
	High	H	[0.332–0.664]
	Very high	VH	[0.498–0.830]
	Excellent	E	[0.664–1.00]

Table 5. List of fuzzy rules of T – FLM

Rule 1:	If	$\eta_{(Ra)}$	is	Small	and	$\eta_{(\Delta L)}$	is	Small	then	MRPI	is	Low
Rule 2:	If	$\eta_{(Ra)}$	is	Medium	and	$\eta_{(\Delta L)}$	is	Small	then	MRPI	is	Low
Rule 3:	If	$\eta_{(Ra)}$	is	High	and	$\eta_{(\Delta L)}$	is	Small	then	MRPI	is	Medium
Rule 4:	If	$\eta_{(Ra)}$	is	Extremely high	and	$\eta_{(\Delta L)}$	is	Small	then	MRPI	is	Medium
Rule 5:	If	$\eta_{(Ra)}$	is	Small	and	$\eta_{(\Delta L)}$	is	Medium	then	MRPI	is	Low
Rule 6:	If	$\eta_{(Ra)}$	is	Medium	and	$\eta_{(\Delta L)}$	is	Medium	then	MRPI	is	Medium
Rule 7:	If	$\eta_{(Ra)}$	is	High	and	$\eta_{(\Delta L)}$	is	Medium	then	MRPI	is	Medium
Rule 8:	If	$\eta_{(Ra)}$	is	Extremely high	and	$\eta_{(\Delta L)}$	is	Medium	then	MRPI	is	High
Rule 9:	If	$\eta_{(Ra)}$	is	Small	and	$\eta_{(\Delta L)}$	is	High	then	MRPI	is	Medium
Rule 10:	If	$\eta_{(Ra)}$	is	Medium	and	$\eta_{(\Delta L)}$	is	High	then	MRPI	is	Medium
Rule 11:	If	$\eta_{(Ra)}$	is	High	and	$\eta_{(\Delta L)}$	is	High	then	MRPI	is	High
Rule 12:	If	$\eta_{(Ra)}$	is	Extremely high	and	$\eta_{(\Delta L)}$	is	High	then	MRPI	is	Very high
Rule 13:	If	$\eta_{(Ra)}$	is	Small	and	$\eta_{(\Delta L)}$	is	Extremely high	then	MRPI	is	Medium
Rule 14:	If	$\eta_{(Ra)}$	is	Medium	and	$\eta_{(\Delta L)}$	is	Extremely high	then	MRPI	is	High
Rule 15:	If	$\eta_{(Ra)}$	is	High	and	$\eta_{(\Delta L)}$	is	Extremely high	then	MRPI	is	Very high
Rule 16:	If	$\eta_{(Ra)}$	is	Extremely high	and	$\eta_{(\Delta L)}$	is	Extremely high	then	MRPI	is	Excellent

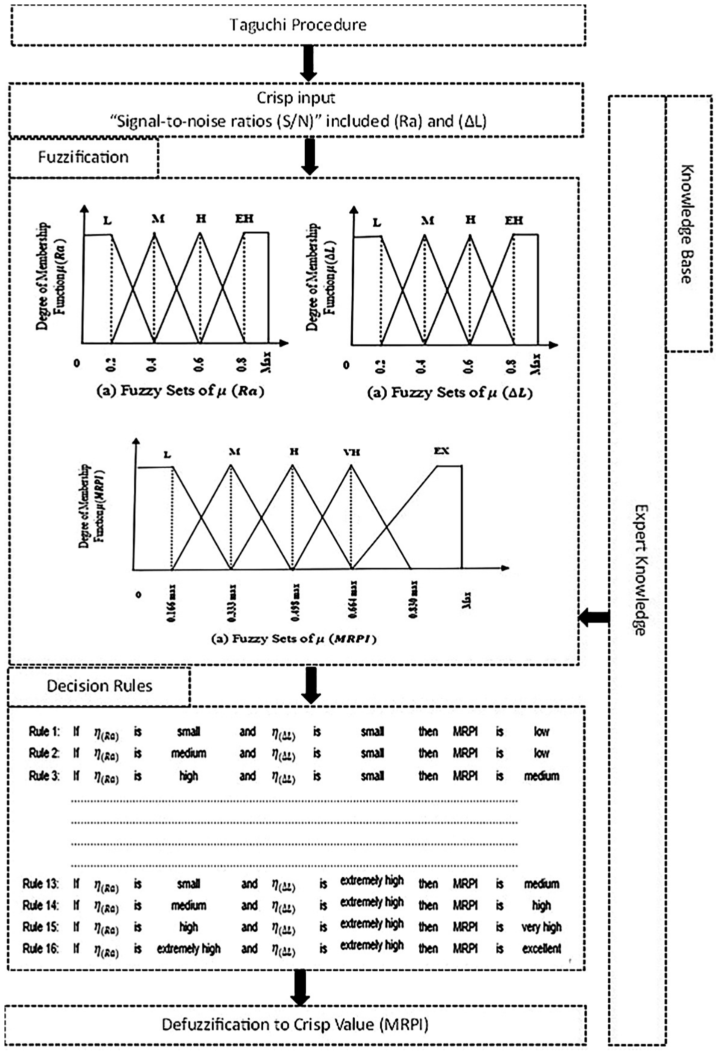

Figure 3. Outline of the developed T-FLM

Taguchi–fuzzy framework are rigorously detailed below, establishing a transparent basis for the multi-objective optimization results.

Model analysis

The experimental results of runs and their corresponding standard deviation are tabulated in Tables 6 and 7, whereas the results of S/N ratio values are presented in Table 8. The results revealed significant variations in Ra, highlighting a strong association with their respective S/N ratio across the different surfaces. Specifically, the horizontal surface exhibited the lowest Ra value (1.444 μm) compared to the rotational surface (9.032 μm), which recorded the highest value. This deviation reflects the high sensitivity of the deposition process to the surface inclination angle; this behavior is primarily attributed to the staircase effect. In particular, the adverse effects of a larger layer thickness become more pronounced as the step height and contact area fluctuate with the surface slope. This is evident from the wide range of S/N ratio values; for instance, the S/N ratio decreased from -3.191 dB for the horizontal orientation to -19.115 dB for the rotational orientation within the same optimal experiment (run 25), as shown in Figure 4. The experimental results revealed a noticeable disparity in ΔL across the studied surface orientations under the same manufacturing parameters. To illustrate, the deviation in dimensional accuracy of the inclined surface consistently tends to be larger than that of the other surfaces. For instance, in experiment 20, while both the rotational and horizontal surfaces exhibited minimal ΔL values of 0.128 mm and 0.306 mm, respectively, the inclined surface exhibited a higher ΔL values (4.734 mm). Furthermore, the results of experiment 16 indicated that the vertical surface exhibited the minimum

Table 6. Experimental results of Ra and their corresponding standard deviation

Exp.	Measurements of Ra (μm)							
	S_R	STDEV	SH	STDEV	SV	STDEV	SI	STDEV
1	5.886	0.118	3.750	0.075	6.013	0.12	6.030	0.121
2	6.642	0.133	3.035	0.061	5.826	0.117	6.100	0.122
3	6.223	0.124	2.366	0.047	7.150	0.143	8.84	0.177
4	6.214	0.124	2.957	0.059	6.481	0.13	8.001	0.16
5	6.176	0.124	3.533	0.071	5.012	0.1	7.080	0.142
6	6.016	0.12	3.803	0.076	7.248	0.145	3.269	0.065
7	5.966	0.119	4.063	0.081	6.257	0.125	4.030	0.081
8	4.012	0.08	3.283	0.066	1.688	0.034	3.353	0.067
9	4.952	0.099	4.470	0.089	1.746	0.035	5.150	0.103
10	8.242	0.165	4.652	0.093	6.622	0.132	8.890	0.178
11	8.353	0.167	4.189	0.084	8.241	0.165	7.630	0.153
12	5.199	0.104	4.154	0.083	5.740	0.115	5.421	0.108
13	7.001	0.14	2.572	0.051	4.345	0.087	6.347	0.127
14	8.271	0.165	1.780	0.036	2.797	0.056	8.546	0.171
15	7.782	0.156	1.616	0.032	7.431	0.149	6.891	0.138
16	6.913	0.138	4.727	0.095	6.455	0.129	9.214	0.184
17	8.057	0.161	2.850	0.057	9.079	0.182	9.358	0.187
18	8.240	0.165	2.850	0.057	9.079	0.182	10.305	0.206
19	7.535	0.151	2.355	0.047	6.077	0.122	5.382	0.108
20	8.869	0.177	2.472	0.049	8.523	0.17	8.002	0.160
21	8.078	0.162	2.819	0.056	8.687	0.174	11.306	0.226
22	7.352	0.147	1.994	0.04	5.499	0.11	8.369	0.167
23	7.325	0.147	3.197	0.064	7.502	0.15	7.952	0.159
24	7.821	0.156	2.98	0.06	8.922	0.178	10.427	0.209
25	9.032	0.181	1.444	0.029	3.415	0.068	3.781	0.076
26	8.925	0.179	1.660	0.033	7.247	0.145	7.25	0.145
27	5.234	0.105	2.428	0.049	5.915	0.118	9.873	0.197

ΔL value (0.071 mm) compared to the inclined surface (2.513 mm). This distinct variation highlights an orientation-dependent behavior, leading to anisotropic surface accuracy, as illustrated in Figure 5. This variation is typically attributed to the staircase effect and thermal gradient arising during the solidification process, both of which disrupt dimensional stability at specific angles. This provides strong evidence validating that a traditional optimization approach is insufficient for complex geometries, thereby justifying the necessity of developing an advanced model to accurately evaluate surface quality in such parts. By considering multi-directional surface quality variations, the proposed model achieves greater integrity and uniformity in FDM components. Consequently, this study confirms that the hybrid model (T-FLM) is vital for ensuring uniformity of surface quality regardless of the part orientation.

Following the experimental phase, T-FLM was implemented to evaluate the manufacturing responses. The distinct advantage of this model lies in its capability to aggregate multiple optimization responses into a single, realistic index. Furthermore, it determines the combination of optimal factor levels that simultaneously satisfy all targeted performance objectives. Table 9 listed the obtained MRPI results for both the traditional Taguchi approach and T–FLM. Within this framework, a larger multi-response performance index indicates a smaller variance of the performance characteristics around the desired value.

As illustrated by the graphical trends in Figure 6, where variations in the MRPI values across the experimental runs are further

Table 7. Experimental results of ΔL and their corresponding standard deviation

Exp.	Measurements of ΔL (mm)							
	S_R	STDEV	S_H	STDEV	S_V	STDEV	S_I	STDEV
1	1.862	0.037	0.587	0.012	1.980	0.04	1.106	0.022
2	0.750	0.015	0.643	0.013	0.932	0.019	2.366	0.047
3	0.982	0.02	0.767	0.015	0.759	0.015	5.291	0.106
4	0.604	0.012	0.660	0.013	1.025	0.02	2.911	0.058
5	0.542	0.011	0.334	0.007	1.140	0.023	1.063	0.021
6	0.795	0.016	0.578	0.012	1.251	0.025	0.407	0.008
7	1.192	0.024	0.699	0.014	0.468	0.009	2.005	0.04
8	1.078	0.022	0.784	0.016	0.701	0.014	1.705	0.034
9	0.908	0.018	0.654	0.013	0.211	0.004	3.371	0.067
10	0.945	0.019	1.172	0.023	0.176	0.004	0.913	0.018
11	1.752	0.035	0.466	0.009	1.105	0.022	2.971	0.059
12	1.115	0.022	1.115	0.022	0.252	0.005	3.168	0.063
13	0.770	0.015	0.598	0.012	0.147	0.003	3.564	0.071
14	0.410	0.008	0.346	0.007	0.468	0.009	3.211	0.064
15	1.058	0.021	0.446	0.009	0.159	0.003	4.740	0.095
16	0.852	0.017	0.727	0.015	0.071	0.001	2.513	0.05
17	0.897	0.018	0.727	0.015	0.135	0.003	3.879	0.078
18	1.115	0.022	0.908	0.018	0.387	0.008	2.543	0.051
19	1.030	0.021	0.756	0.015	0.854	0.017	2.366	0.047
20	0.128	0.003	0.306	0.006	1.025	0.02	4.734	0.095
21	1.010	0.02	0.663	0.013	0.468	0.009	5.291	0.106
22	0.767	0.015	0.965	0.019	1.010	0.02	5.785	0.116
23	0.671	0.013	0.559	0.011	1.123	0.022	5.711	0.114
24	1.477	0.03	0.767	0.015	1.180	0.024	3.848	0.077
25	1.067	0.021	0.860	0.017	0.439	0.009	1.523	0.03
26	0.251	0.005	0.214	0.004	0.633	0.013	4.364	0.087
27	0.945	0.019	0.727	0.015	0.817	0.016	3.106	0.062

detailed and quantified in Table 10, a comprehensive comparison of each individual experiment was conducted. The findings emphasize the enhanced capability and superiority of the proposed model relative to the traditional Taguchi method for all investigated surfaces. This is further evidenced by the consistent achievement of elevated MRPI values across the 27 experimental runs, accompanied by a noticeable mean improvement of 15.2%, as depicted in Figure 7. Furthermore, the obtained results indicate a clear reduction in the standard deviation of the overall surface quality, which was successfully validated across approximately 78% of the experimental runs, as illustrated in Figure 8. To demonstrate the inherent stability of the developed model, the descriptive statistics of all evaluated surfaces are shown in Table 11. The empirical findings reveal that the coefficient of variation (CV) and standard error (SE mean) remain consistently low across all experimental runs, ranging from (16.30% to 37.12%) and (0.018 to 0.029) respectively. This uniformity observed across repeated trials, evidenced by the narrowed dispersion of MRPI values, confirms the robustness of the developed model. This stability indicates that the proposed model provides superior control over the inherent variable of FDM printing, especially when dealing with complex geometries. Finally, the obtained results indicate that the developed fuzzy model is less sensitive to changing surfaces orientations; thereby, demonstrating its ability to effectively and reliably minimize the staircase effect and thermal gradient during solidification inherent in the printing process.

Table 8. S/N ratio of surface roughness and dimension accuracy for surface orientations

Exp.	S/N ratio of Ra (dB)				S/N ratio of ΔL (dB)			
	S_R	S_H	S_V	S_I	S_R	S_H	S_V	S_I
1	-15.390	-11.4806	-15.5818	-15.6063	-5.3987	4.6308	-5.9316	-0.8737
2	-16.440	-9.6432	-15.3074	-15.7066	2.4985	3.8358	0.6079	-7.4797
3	-15.880	-7.4803	-17.0861	-18.9290	0.1598	2.3047	2.3963	-14.4714
4	-15.8674	-9.4170	-16.2328	-18.0629	4.3847	3.6107	-0.2118	-9.2809
5	-15.8141	-10.9629	-14.0002	-17.0007	5.3231	9.5134	-1.1366	-0.5342
6	-15.5862	-11.6025	-17.2044	-10.2883	1.9909	4.7566	-1.9434	7.8064
7	-15.5137	-12.1769	-15.9273	-12.1061	-1.5242	3.1067	6.5880	-6.0422
8	-12.0672	-10.3254	-4.5474	-10.5087	-0.6537	2.1151	3.0865	-4.6359
9	-13.8956	-13.0062	-4.8409	-14.2361	0.8366	3.6851	13.5013	-10.5552
10	-18.3207	-13.3528	-16.4198	-18.9780	0.4918	-1.3779	15.0819	0.7866
11	-18.4368	-12.4422	-18.3196	-17.6505	-4.8727	6.6313	-0.8696	-9.4577
12	-14.3184	-12.3693	-15.1782	-14.6816	-0.9461	-0.9461	11.9616	-10.0159
13	-16.9032	-8.2054	-12.7598	-16.0514	2.2728	4.4660	16.6629	-11.0390
14	-18.3512	-5.0084	-8.9338	-18.6353	7.7442	9.2276	6.5880	-10.1338
15	-17.8218	-4.1688	-17.4209	-16.7656	-0.4922	7.0050	15.9679	-13.5161
16	-16.7933	-13.4917	-16.1979	-19.2890	1.3949	2.7636	23.0315	-8.0040
17	-18.1235	-9.0969	-19.1608	-19.4237	0.9455	2.7636	17.3862	-11.7734
18	-18.3185	-9.0969	-19.1608	-20.2610	-0.9461	0.8366	8.2518	-8.1062
19	-17.5417	-7.4398	-15.6738	-14.6189	-0.2563	2.4334	1.3678	-7.4797
20	-18.9575	-7.8610	-18.6118	-18.0640	17.8820	10.2716	-0.2118	-13.5040
21	-18.1461	-9.0019	-18.7774	-21.0662	-0.0873	3.5737	6.5880	-14.4714
22	-17.3281	-5.9945	-14.8057	-18.4535	2.3047	0.3115	-0.0873	-15.2460
23	-17.2962	-10.0949	-17.5035	-18.0095	3.4637	5.0571	-1.0041	-15.1345
24	-17.8652	-9.4843	-19.0092	-20.3632	-3.3879	2.3047	-1.4378	-11.7048
25	-19.1157	-3.1913	-10.6678	-11.5521	-0.5618	1.3089	7.1460	-3.6526
26	-19.0122	-4.4022	-17.2032	-17.2068	12.0195	13.3776	3.9665	-12.7983
27	-14.3767	-7.7050	-15.4391	-19.8890	0.4918	2.7636	1.7577	-9.8445

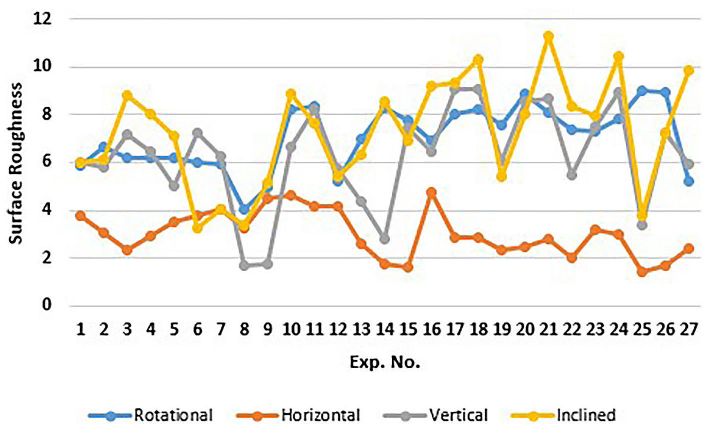

Figure 4. Variation of surface roughness (Ra) across different surface orientations for the 27 experimental runs

Analysis of variance test

The relative impact of process parameters was identified by the Analysis of Variance test (ANOVA). As clarified Table 12, print speed and nozzle temperature have the greatest impact on the uniformity of surface quality of 3D printed results at 31.146% and 17.1 respectively, whereas the top/bottom layer numbers demonstrate a clear lack of statistically significant effect on the target response with P-value (0.397) and contributes (3.783%) to the total variance. On the other hand, the layer thickness (9.463%) and bed temperature (7.589%) were

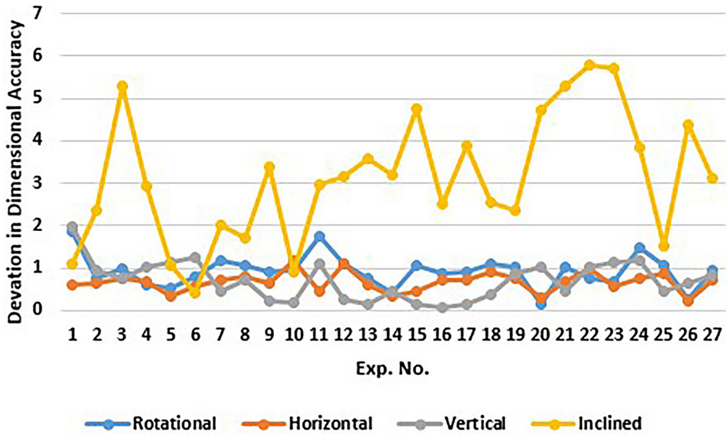

Figure 5. Variation of deviation in dimensional accuracy (ΔL) across different surface orientations for the 27 experimental runs

Table 9. Summarization of MRPI results for Taguchi and T-FLM

Exp. No.	MRPI Taguchi				MRPI T-FLM			
	S_R	S_H	S_V	S_I	S_R	S_H	S_V	S_I
1	0.287	0.528	0.275	0.340	0.580	0.545	0.460	0.546
2	0.361	0.569	0.368	0.251	0.673	0.512	0.750	0.597
3	0.346	0.609	0.342	0.070	0.522	0.513	0.640	0.250
4	0.402	0.572	0.332	0.162	0.513	0.436	0.696	0.265
5	0.416	0.606	0.382	0.306	0.617	0.601	0.450	0.553
6	0.378	0.526	0.282	0.603	0.447	0.550	0.642	0.750
7	0.335	0.488	0.429	0.371	0.541	0.696	0.725	0.558
8	0.442	0.527	0.702	0.434	0.650	0.696	0.750	0.511
9	0.411	0.473	0.829	0.252	0.755	0.633	0.801	0.408
10	0.282	0.397	0.526	0.268	0.578	0.477	0.625	0.515
11	0.209	0.527	0.265	0.171	0.412	0.330	0.373	0.374
12	0.376	0.430	0.520	0.247	0.650	0.471	0.750	0.422
13	0.345	0.617	0.649	0.195	0.649	0.426	0.750	0.302
14	0.376	0.769	0.625	0.135	0.617	0.733	0.750	0.498
15	0.283	0.763	0.510	0.143	0.306	0.708	0.625	0.350
16	0.337	0.447	0.636	0.144	0.758	0.433	0.625	0.339
17	0.294	0.570	0.480	0.091	0.592	0.493	0.500	0.250
18	0.264	0.545	0.360	0.116	0.573	0.543	0.500	0.342
19	0.294	0.612	0.368	0.282	0.623	0.515	0.539	0.409
20	0.492	0.703	0.265	0.107	0.578	0.825	0.553	0.450
21	0.280	0.583	0.349	0.010	0.586	0.458	0.560	0.259
22	0.334	0.625	0.373	0.073	0.632	0.648	0.450	0.250
23	0.350	0.572	0.286	0.087	0.626	0.349	0.625	0.250
24	0.244	0.553	0.238	0.066	0.603	0.484	0.510	0.250
25	0.246	0.716	0.583	0.418	0.500	0.204	0.750	0.744
26	0.414	0.840	0.359	0.140	0.628	0.733	0.226	0.286
27	0.393	0.609	0.380	0.103	0.550	0.768	0.350	0.250

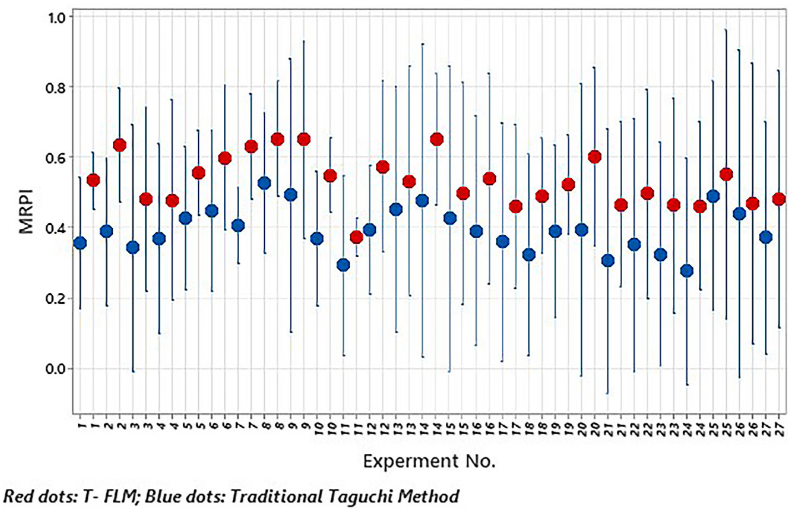

Figure 6. MRPI values comparison between the Taguchi method and T-FLM for individual experiments

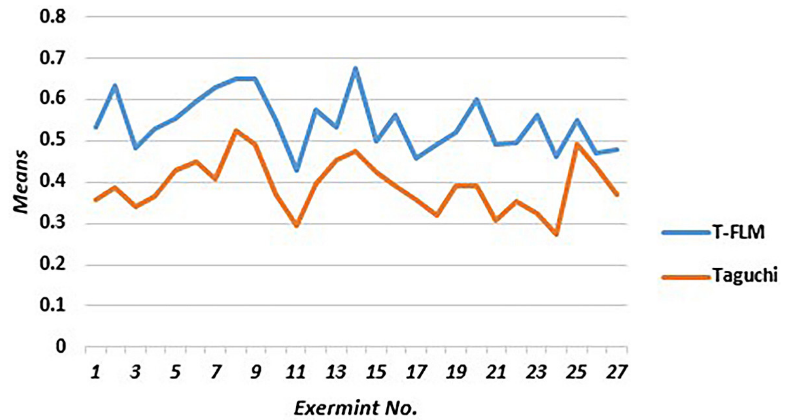

Figure 7. Difference in MRPI means between the Taguchi method and T-FLM for each experiment

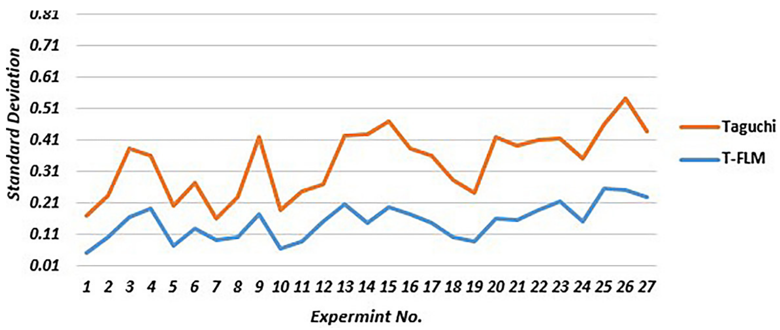

Figure 8. Difference in MRPI standard deviation between Taguchi method and T-FLM for each experiment

not statistically major effects on the responses under the tested conditions. Interestingly, layer thickness and bed temperature have marginal P-value of (0.118) and (0.173) respectively; these marginal values refer to an underlying physical impact that might become noticeable if their operational limits are extended.

Confirmation tests

To verify the improvement of the performance characteristic using the optimal level of the process parameters, it is necessary to carry out a confirmation test. Since the experimental design is orthogonal, it is possible to separate the effect

Table 10. Statistical analysis and their % improvement of MRPI results

Exp. No.	Taguchi Method		T-FLM		Improvement	
	S.D.	Mean	S.D.	Mean	(S.D.)	(Mean)
1.	0.117	0.358	0.051	0.533	0.066	0.175
2.	0.132	0.387	0.102	0.633	0.030	0.246
3.	0.220	0.342	0.165	0.481	0.055	0.140
4.	0.170	0.367	0.191	0.528	-0.021	0.161
5.	0.128	0.428	0.075	0.555	0.052	0.128
6.	0.144	0.447	0.129	0.597	0.015	0.150
7.	0.067	0.406	0.094	0.630	-0.027	0.224
8.	0.124	0.526	0.102	0.652	0.022	0.126
9.	0.244	0.491	0.176	0.649	0.068	0.158
10.	0.120	0.368	0.066	0.549	0.054	0.181
11.	0.161	0.293	0.088	0.429	0.073	0.136
12.	0.114	0.393	0.153	0.573	-0.039	0.180
13.	0.219	0.452	0.204	0.532	0.014	0.080
14.	0.279	0.476	0.148	0.675	0.132	0.198
15.	0.272	0.425	0.199	0.497	0.072	0.073
16.	0.206	0.391	0.176	0.564	0.030	0.173
17.	0.212	0.359	0.146	0.459	0.066	0.100
18.	0.180	0.321	0.103	0.490	0.077	0.168
19.	0.153	0.389	0.088	0.522	0.065	0.133
20.	0.261	0.392	0.159	0.602	0.102	0.210
21.	0.236	0.306	0.155	0.491	0.081	0.185
22.	0.226	0.351	0.186	0.495	0.040	0.144
23.	0.200	0.324	0.216	0.563	-0.016	0.239
24.	0.203	0.275	0.150	0.462	0.053	0.187
25.	0.204	0.491	0.258	0.550	-0.054	0.059
26.	0.293	0.438	0.250	0.468	0.043	0.030
27.	0.207	0.371	0.229	0.480	-0.022	0.108

Table 11. Summary of descriptive statistical analysis

MRPI value of T- FLM	Mean	SE	CV
SR	0.5836	0.0183	16.30
SH	0.5474	0.0282	26.79
SV	0.5916	0.0282	24.77
SI	0.4065	0.0290	37.12

of each printing parameter at different levels. For instance, as outlined in Table 3, the mean of MRPI for layer thickness at levels 1, 2, and 3 is determined by averaging the indices of experiments 1 to 9, 10 to 18, and 19 to 27, respectively. In a similar manner, the mean MRPI values for the remaining control factors are calculated by grouping the corresponding experimental runs that share the same level setting, Table 13 summarized the main effects of mean MRPI for each level of the printing parameters, the larger MRPI is the smaller various of the performance characteristics around the desired value. The optimum factor levels A_1, B_3, C_3, D_3, and E_2 were obtained from the main effect plot of MRPI, as shown in Figure 9.

The experiment was conducted by taking an initial set of process parameter combination beyond experiment layout. It was conducted using the initial FDM parameter setting for A_2, B_1, C_1, D_1, and E_3. The responses, including Ra and ΔL

Table 12. Results of the analysis of variance

Symbol	FDM Parameters	DF	Sum of squares	Mean of squares	F-Value	P-Value	Contribution (%)
A	Layer thickness (mm)	2	0.009896	0.004948	2.45	0.118	9.463
B	Nozzle temp. (˚C)	2	0.017883	0.008942	4.42	0.030	17.100
C	Print speed (mm/sec)	2	0.032573	0.016286	8.06	0.004	31.146
D	Bed temp. (˚C)	2	0.007937	0.003968	1.96	0.173	7.589
E	Top/bottom layer number	2	0.003956	0.001978	0.98	0.397	3.783
Error		16	0.032336	0.002021			
Total		26					

Table 13. Main effects of mean MRPI at different parameter levels

Symbol	FDM Parameters	Mean MRPI			
		Level 1	Level 2	Level 3	Max-Min
A	Layer thickness (mm)	0.5842	0.5298	0.5148	0.069
B	Nozzle temp. (˚C)	0.5348	0.5449	0.5491	0.014
C	Print speed (mm/sec)	0.52	0.5254	0.5833	0.063
D	Bed Temp. (˚C)	0.5388	0.5342	0.5558	0.022
E	Top/bottom layer No. (#)	0.5448	0.5596	0.5244	0.035
Total mean MRPI = 0.543					

were measured three times, and the mean was calculated and taken as the corresponding value of these responses, which was (6.954 μm,1.485 mm), (4.154 μm, 0.945 mm), (6.557 μm, 0.561 mm), and (7.032 μm, 2.214 mm) respectively. MRPI is predicted using the optimal level of the process parameters based on Equation 8 [23], where η_m is the total mean of MRPI, $\bar{\eta}_i$ is the mean of MRPI at the optimal level, and q is the number of the process parameters that significantly affect the MRPI characteristics. The results of the confirmation experiment conducted using the initial and the best possible FDM parameters are shown in Table 14. Considering the comparison between the experimental and predicted values, the absolute percentage error is calculated as 5.98%, which is satisfactory and complies with the threshold criteria for highly accurate prediction (≤ 10%). Thereby, the developed model is capable of enhancing the uniformity of surface quality in terms of MRPI to a justifiable degree of accuracy.

$$\hat{\eta} = \eta_m + \sum_{i=1}^{q}(\bar{\eta}_i - \eta_m) \tag{8}$$

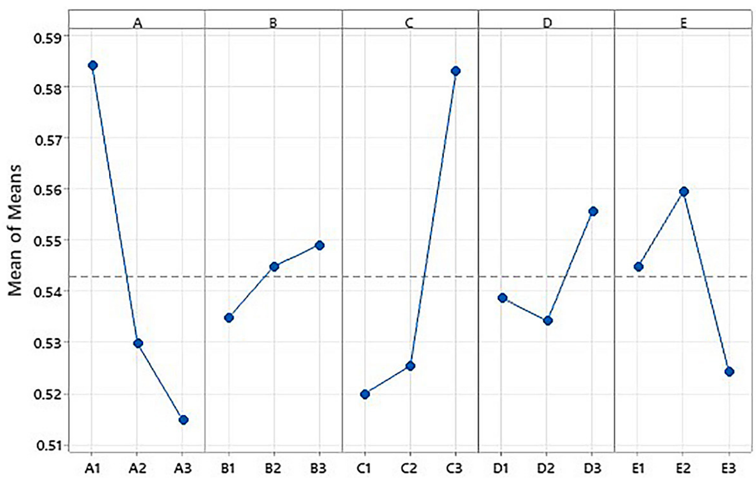

Figure 9. Main parameter effect plot (data mean) for MRPI

Table 14. Results of the confirmation experiment

Description	Initial FDM parameters				Optimal FDM parameters				
					Prediction	Experiment			
Levels	A_2 B_1 C_1 D_1 E_3				A_1 B_3 C_3 D_3 E_2	A_1 B_3 C_3 D_3 E_2			
	SR	SH	SV	SI		SR	SH	SV	SI
Ra (μm)	6.954	4.154	6.557	7.032		3.296	2.668	4.509	5.727
ΔL (mm)	1.485	0.445	0.561	2.214		0.743	0.153	0.368	1.370
MRPI	0.351				0.660	0.702			
Improvement MRPI = 0.351									

CONCLUSIONS

The purpose of this study was to investigate the influence of surface orientation on the uniformity of surface quality in FDM-fabricated components. The investigation involved the characterization of four surfaces evaluated across rotational, horizontal, vertical, and inclined orientations. The developed model was based on integrating the Taguchi approach and fuzzy logic model to identify the optimal process parameters for 3D printing ensuring uniformity across various surface orientations. The Taguchi approach was used to determine the initial 3D print input parameters to minimize surface roughness and deviation in dimensional accuracy values as a single objective, denoted by S/N ratio. The hybrid Taguchi – fuzzy logic model (T–FLM) was developed as a robust experimental framework to evaluate the performance, which can also be extended to handle multi-objective optimization via the multi–response performance index (MRPI), specifically with lower surface roughness (Ra) and deviation in dimensional accuracy (ΔL). This framework effectively addressed incomplete and imprecise information, which typically challenges conventional probability theory. The obtained results prove the statistical superiority of the hybrid T–FLM over the traditional Taguchi approach. This was corroborated across all surface orientations during quantitative evaluation, where fuzzy model yields significantly better attributes in central tendency and variability criteria. It was evidenced during statistical analysis that the fuzzy method was successfully employed to improve the mean and standard deviation values of the overall surface quality. Finally, the validity of the optimized parameters was successfully verified through an experimental confirmation test. Consequently, the hybrid model was validated to effectively enhance the surface integrity uniformity of FDM parts. While the model shows significant improvements, its application remains subjected to the specific design space and material properties explored during the experimental study. Thus, the effect of the proposed hybrid model should be further investigated on a wider range of materials, such as higher performance polymers (PEEK), to verify its versatility in practical application.

REFERENCES

1. Ngo T.D., Kashani A., Imbalzano G., Nguyen K.T.Q., and Hui D. Additive manufacturing (3D Printing): A review of materials, methods, applications and challenges. Composites Part B: Engineering. 2018; 143: 172–196. https://doi.org/10.1016/j.compositesb.2018.02.012
2. Wicaksono M. B. and Nugraha F. K. A. Optimization of 3D printing parameters using the taguchi method to improve dimensional precision. Jurnal Teknologi. 2022; 12(2): 13–18. https://doi.org/10.35134/jitekin.v12i2.72
3. Gopsill J.A., Shindler J., and Hicks B.J. Using finite element analysis to influence the infill design of fused deposition modelled parts. Prog Addit Manuf. 2018; 3: 145–163. https://doi.org/10.1007/s40964-017-0034-y
4. Fafenrot S., Grimmelsmann N., Wortmann M., and Ehrmann A. Three-dimensional (3D) printing of polymer-metal hybrid materials by fused deposition modeling. Materials. 2017; 10(10): 1199. https://doi.org/10.3390/ma10101199
5. Shiaa W. Q., Jabbar R., and Aufy S. A. Design and evaluate a customized PEEK implant for large skull defect reconstruction. Production Engineering Archives. 2025; 31(4): 517–525. https://doi.org/10.30657/pea.2025.31.48
6. El-Zathry N.E., El-Attar T., Sabry I., et al. Fused deposition modeling component quality enhancement by experimental investigation and ANN prediction. Int J Interact Des Manuf. 2026; 20: 1085–1108. https://doi.org/10.1007/s12008-025-02430-3
7. Sağbaş B., Poyraz O., and Durakbasa N. A comparative study on precision metrology systems for additive manufacturing. International Journal of 3D Printing

Technologies and Digital Industry. 2023; 7: 114–123. https://doi.org/10.46519/ij3dptdi.1206753

8. Marifah S.L., Saputri U.S., and Permadi D.D. Systematic literature review: 3D printing technology for sustainable construction innovation. Eng. Proc. 2025; 107(1): 93. https://doi.org/10.3390/engproc2025107093
9. Wei X., Zhang S., Sun L., Zhao X., Sun M., Yu R., Zhou X., and Li Y. Geometric accuracy and dimensional precision in 3D printing-based gear manufacturing: A study on interchangeability and forming precision. Polymers. 2025; 17(3): 416. https://doi.org/10.3390/polym17030416
10. Kmiecik-Sołtysiak U., Szczygieł P., Michta D., and Gałczyńska K. Analysis of surface topography, dimensional and geometric deviations, and biocidal properties of 3D prints made of thermoplastic-based composites. Materials. 2026; 19(1): 129. https://doi.org/10.3390/ma19010129
11. Salman A.M., Mansour M.M., and Lafta A.M. Optimizing 3D printing processes by applying the Taguchi method for enhanced efficiency. Academic Journal of Manufacturing Engineering. 2025; 23(3): 136–151. https://doi.org/10.5281/zenodo.17217531
12. Sammaiah P., Rushmamanisha K., Praveenadevi N., and Reddy I. R. The Influence of Process Parameters on the Surface Roughness of the 3D Printed Part in FDM Process. International Conference on Recent Advancements in Engineering and Management (ICRAEM). Warangal. India; IOP Conference Series: Materials Science and Engineering. 2020.
13. Trivedi A. and Gurrala P. K. Fuzzy logic based expert system for prediction of tensile strength in Fused Filament Fabrication (FFF) process. Materials Today: Proceedings. 2021; 44(1): 1344-1349. https://doi.org/10.1016/j.matpr.2020.11.391
14. Syed M. A. B., Rhaman Q., Shahriar H. M., and Khan M. M. A. Grey-Taguchi approach to optimize fused deposition modeling process in terms of mechanical properties and dimensional accuracy J. Eng. Res. Innov. Educ. 2022; 4(1): 38–52. https://researchrepository.wvu.edu/grad_scholarship/7
15. Hasdiansah H., Yaqin R. I., Pristiansyah P., Umar M. L., and Priyambodo B. H. FDM-3D printing parameter optimization using Taguchi approach on surface roughness of thermoplastic polyurethane parts. International Journal on Interactive Design and Manufacturing. 2023; (17): 3011–3024, https://doi.org/10.1007/s12008-023-01304-w
16. Deswal S., Kaushik A., Garg R.K., et al. Optimization of fused deposition modelling printing parameters using hybrid GA-fuzzy evolutionary algorithm. Sādhanā. 2024; 49(257). https://doi.org/10.1007/s12046-024-02595-9
17. Abdulridha H. H., Abbas T. F., and Bedan A. S. Investigate the effect of chemical post processing on the surface roughness of fused deposition modeling printed parts. Advances in Science and Technology Research Journal. 2024; 18(2): 47–60. https://doi.org/10.12913/22998624/183528
18. Abeykoon C., Sri-Amphorn P., and Fernando A. Optimization of fused deposition modeling parameters for improved PLA and ABS 3D printed structures. International Journal of Lightweight Materials and Manufacture. 2020; 3(3): 284–29, https://doi.org/10.1016/j.ijlmm.2020.03.003
19. Mani M., Karthikeyan A.G., Kalaiselvan K., Muthusamy P., and Muruganandhan P. Optimization of FDM 3-D printer process parameters for surface roughness and mechanical properties using PLA material. Materials Today: Proceedings. 2022; 66(4): 1926–1931. https://doi.org/10.1016/j.matpr.2022.05.422
20. Al-Wswasi M., Al-Khaleeli W. A., and Aufy, S. A. Implement the artificial neural network concept for predicting the mechanical properties of printed polylactic acid parts. Advances in Science and Technology Research Journal. 2025; 19(5): 73–83. https://doi.org/10.12913/22998624/201463
21. Chandran V., Kalman J., Fayazbakhsh K., and Bougherara H. A comparative study of the tensile properties of compression molded and 3D printed PLA specimens in dry and water saturated conditions, J Mech Sci Technol, May 2021; 35(5): 1977–1985. https://doi.org/10.1007/s12206-021-0415-5
22. Abdulridha H. H. and Abbas T. F. Analysis and investigation the effect of the printing parameters on the mechanical and physical properties of PLA parts fabricated via FDM printing. Advances in Science and Technology Research Journal. 2023; 17(6): 49–62. https://doi.org/10.12913/22998624/173562
23. Padhi S. K., Sahu R. K., Mahapatra S. S., et al. Optimization of fused deposition modeling process parameters using a fuzzy inference system coupled with Taguchi philosophy. Adv. Manuf. 2017; 5: 231–242. https://doi.org/10.1007/s40436-017-0187-4
24. Tunçel O., Tüfekci K., and Kahya Ç. Multi-objective optimization of 3D printing process parameters using gray-based Taguchi for composite PLA parts. Polym Compos. 2024; 45(14): 12870–12884. https://doi.org/10.1002/pc.28674
25. Sánchez R. J., Blas, M. J., Fernández M. B., and Nolasco S. M. Applying a Taguchi-based fuzzy logic approach to optimize hydrothermal pretreatment of canola seeds using multi-response performance index. OCL - Oilseeds and fats, Crops and Lipids. 2021; 28; 8. https://doi.org/10.1051/ocl/2020076
26. Shetty R. and Hegde A. Taguchi based fuzzy logic model for optimisation and prediction of surface roughness during AWJM of DRCUFP composites. Manufacturing Review. 2022; 9(2); https://doi.org/10.1051/mfreview/2021027